Research article

Magnetic fabric of deformed Quaternary sediments: contributions to the understanding of the neotectonic activity in the surroundings of the Aburrá Valley, Central Cordillera, Colombia

Fábrica magnética de sedimentos cuaternarios deformados: contribuciones para entender la actividad neotectónica en los alrededores del Valle de Aburrá, Colombia

Santiago Noriega-Londoño[1], Duván Jaraba[1], María Paula Ruiz[1], María Isabel Marín-Cerón[1], Sergio Andrés Restrepo-Moreno[2, 3]

1. Environmental Geology and Tectonics Research Group, Department of Earth Sciences, Universidad EAFIT, Medellín, Colombia.
2. Department of Geosciences and Environment, Universidad Nacional de Colombia, Medellín, Colombia.
3. Department of Geological Sciences, University of Florida, Gainesville, USA.
Corresponding author: Santiago Noriega-Londoño, santiageo@gmail.com

Abstract

The origin of the Aburrá Valley (AV) is proposed as a set of coalescent tectonic subbasins located along the northern portion of the Central Cordillera of Colombia, the Northern Andes of Colombia. The Itagüí, Medellín, Bello, and Barbosa subbasins have developed between the Romeral Shear Zone (RSZ) and the Antioqueño Batholith starting in the Late Cenozoic. The aim of this study is to contribute to the understanding of the AV neotectonic framework using the anisotropy of magnetic susceptibility (AMS) and structural analysis. For this, we measure the magnetic fabric ellipsoid shape of faulted sediments and compare them with the geometry and kinematics of fault planes to determine their relationship with the present-day stress field and the regional fault architecture. The principal directions of the elongation axes along the La Brizuela and Yarumalito sites were NE-SW, following the magnetic lineation trend and marking a normal displacement with a dextral component. A marked NW-SE magnetic cleavage was found for the La Caimana site along a strike-slip tectonic setting. Holocene ruptures of the principal displacement zone (i.e., the RSZ) and their surroundings, may indicate normal faulting, with fault bends and steps over basins controlled primarily by R´ and P structures. Moreover, the active faults located to the east of the AV indicate post Plio-Pleistocene deformations with normal faulting through 90/80 to 150/70 antithetic faults. This work identifies the AMS technique as a powerful tool, for understanding the neotectonic framework along urban and surrounding areas.

Resumen

El origen del Valle de Aburrá ha sido propuesta como un conjunto de subcuencas tectónicas coalescentes, ubicadas a lo largo de la cordillera Central de Colombia, Andes del Norte de Colombia. Las subcuencas se habían desarrollado entre la zona de Cizalla romeral (ZSR) y el Batolito Antioqueño desde el Cenozoico Tardío. El objetivo de este estudio es contribuir a la comprensión del marco tectónico del Valle de Aburrá, mediante el uso de la anisotropía de la susceptibilidad magnética y el análisis estructural. Para ello, medimos la forma elipsoide de la tela magnética de los sedimentos con fallas y la comparamos con la geometría y cinemática de los planos de falla para determinar su relación con el campo de tensión actual y la arquitectura de fallas regionales. Las principales direcciones de los ejes de elongación a lo largo de los sitios de La Brizuela y Yarumalito fueron NE-SW, paralelo a la tendencia de lineación magnética y marcan un desplazamiento normal con componente dextral. Se encontró, además, una marcada escisión magnética NW-SE para el sitio de La Caimana a lo largo de un entorno tectónico de deslizamiento de golpe. Las rupturas del Holoceno de la zona de desplazamiento principal (es decir, la RSZ) y sus alrededores, pueden indicar fallas normales, con curvas de falla y paso sobre cuencas controladas principalmente por estructuras R' y P. Además, las fallas activas ubicadas al este del AV indican deformaciones posteriores al Plio-Pleistoceno con fallas normales a través de fallas antitéticas de 90/80 a 150/70. Este trabajo pone de presente la técnica de la anisotropía de la susceptibilidad magnética como una herramienta útil en la comprensión del marco neotectónico a lo largo de las áreas urbanas y circundantes.

Palabras clave: Tectónica activa, zona de cizallamiento Romeral, anisotropía de susceptibilidad magnética, elipsoide de deformación, peligro sísmico, Andes colombianos.

1. Introduction

Documenting the geometry, kinematic and last time of displacement of faults is key for neotectonic studies and seismic hazard assessment. Neotectonics is responsible for understanding the current tectonic deformation framework of a region to characterize the long-term history of active faults, i.e., faults that have registered earthquakes in the recent geological past (Stewart, 2005). Thus, neotectonic studies are classically based on fault-related geomorphic expressions, the spatial distribution of recent deposits with stratigraphic evidence of deformation, and historical and instrumental seismicity. They constitute the essential elements to characterize the history and recent activity of seismogenic faults (Burbank and Anderson, 2011; McCalpin, 2013). The minerals within the fault zone and the immediate surroundings can be mechanically rotated and reoriented, accommodating the equilibrium conditions that mark rupture plane orientations (Passchier and Trouw, 2005). This imprints a particular fabric on the deformed minerals, with particular geometry and kinematics, due to the superimposed strain field (Parés and Pluijm, 2002).

The anisotropy of magnetic susceptibility (AMS) is a geometric representation of the shape of the magnetic fabric in the ellipsoid as a function of the magnetic susceptibility distribution (tensor defined by the $k_1 \geq k_2 \geq k_3$ axis) of minerals in a sample (Jelinek, 1981). The magnetic susceptibility (k) refers to the ability of minerals to acquire induced magnetization (Bilardello, 2016; Borradaile, 1988), then the shape of the magnetic fabric ellipsoid represents how paramagnetic and magnetic minerals are distributed along space (Parés, 2015).

The Aburrá Valley (AV) is located between the Antioqueño Plateau (AP) (Arias, 1996; Restrepo-Moreno et al., 2009) and the Romeral shear zone (RSZ) (Vinasco, 2019) with an 8-25 km wide fault zone that comprises various fault traces (Correa-Martínez et al., 2020). These two first-order landforms indicate that the AV is the product of coupled tectonic and erosive processes. However, the origin and evolution of this valley (e.g., clearly tectonic and/or erosive hypotheses) have been a subject of broad scientific discussion (e.g., Aristizábal et al., 2004; Aristizábal and Yokota, 2008; García, 2006; Hermelin, 1982, 1992; Rendón, 2003; Rendón et al., 2006). However, recent tectonic geomorphology and geophysics studies demonstrate that the AV is a tectonic valley influenced by regional faults (Rendón, 2003), covered by extensive Quaternary and Pliocene deposits, which filled independent pull-apart subbasins, today grouped along the Medellín-Porce drainage system.

Fault-related neotectonic expressions are associated with changes along the river profile, the morphology of each tectonic subbasin, and the occurrence of alluvial and hill slope deposits with evidence of tectonic deformation.

Faults covered by sediments of relatively well-known ages are fundamental in neotectonic investigation because i) they allow estimating a relative age of the deformation, and ii) they can reproduce the geometry and kinematics of these faults as the tectonic structures and the magnetic fabric tend to be parallel to subparallel. Opportunities to characterize active faults by the analysis of deformed sediment demonstrate the crucial role of Quaternary deposits as key for basic seismic hazards.

The main objective of this project is to contribute to the understanding of the neotectonic activity in the surroundings of the AV, Central Cordillera, Colombia, based on the magnetic fabric of deformed Quaternary sediments. For this reason, the magnetic susceptibility anisotropy (AMS) technique was used to constrain the sediment deformation along the AV and

surroundings to characterize the magnetic fabric and deformation ellipsoids along active faults. With these data, we search to contribute to updating the tectonic evolution models of this portion of the Central Cordillera, and the evaluation of the seismic hazards in the Aburrá metropolitan area.

2. Study site

The AV is in the north Central Cordillera and is surrounded by the RSZ on its western side and the Antioqueño Batholith in the east and north east (Figure 1). The RSZ represents a major long-term regional structure (e.g., Chicangana, 2005; Correa-Martínez et al., 2020; Ego et al., 1996; Vinasco, 2019; Vinasco and Cordani, 2012), and the Antioqueño Batholith, is one of the major Cretaceous granitic bodies of the Central Cordillera (more than 8000 km² exposed area), which can be considered as an analogous to a backstop (i.e., large rigid block in response to deformation (Rodríguez et al., 2005; Restrepo-Mo-
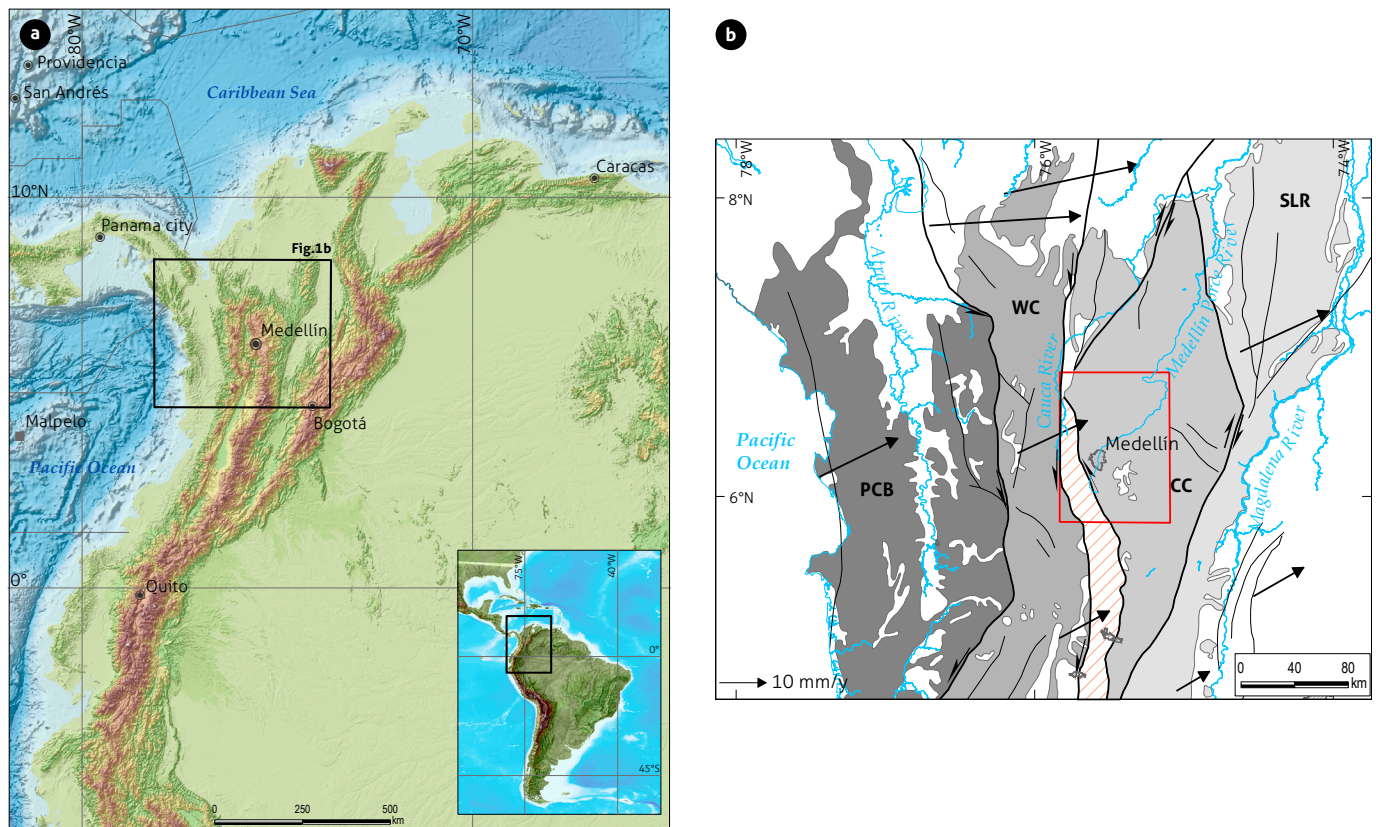
Figure 1. Study site location
a) The Colombian Andes in the South American and Andean context.. b) Simplified map of Northwestern Colombian Andes with main active faults at both sides of the Central Cordillera, and location of the AV. The black arrow indicates the GPS vectors relative to stable South America after Mora-Páez et al. (2020). CC = Central Cordillera, SLR = San Lucas Range, PCB = Panamá-Chocó Block, WC = Western Cordillera.

reno et al., 2009). Therefore, the AV location becomes vital to understanding the tectonic stress transfer and strain partition in relation to landscape response to late Andean orogenic pulses. The present day plate tectonic regime of the Northern Andean belt is dominated by oblique convergence of the Nazca, Caribbean and South American plates that control the behavior of major active faults and seismogenic faults in the region (Costa et al., 2020; Veloza et al., 2012). Understanding the patterns of AV landscape evolution is essential for the improvement of natural hazard assessments and successful land management strategies.

Multiple tectonic and geomorphological models of AV evolution have been proposed in recent decades (e.g., Álvarez et al., 1984; Arbeláez, 2019; Arboleda et al., 2019; Aristizábal et al., 2004; Aristizábal and Yokota, 2008; Botero, 1963; García, 2006; Henao Casas and Monsalve, 2017; Hermelin, 1982; In-

tegral, 1982, 2000; Rendón, 2003; Rendón et al., 2006; SGM, 2002; Shlemon, 1979). All these proposed models coincide with the relevance of climate and tectonic forcing processes in AV development, at least since the Late Pliocene, but the roles of mechanisms and forcing processes differ considerably.

The tectonic configuration of pull-apart basin, push-up blocks and erosive processes along the AV have been proposed partially by many authors (e.g., Botero, 1963; Hermelin, 1982) (Figure 2). Additionally, Rendón (2003), and Rendón et al. (2006) contributed to this hypothesis by integrating morphotectonic, morphostratigraphic, geophysical and geochronologic techniques demonstrating that the AV is the result of the merging of different ancient tectonic subbasins that have been active since at least Pliocene times (Henao Casas and Monsalve, 2017; Rendón et al., 2006; Toro, 1999; Toro et al., 2006). RSZ dynamics and the most recent phases of Andean Orogeny defi-
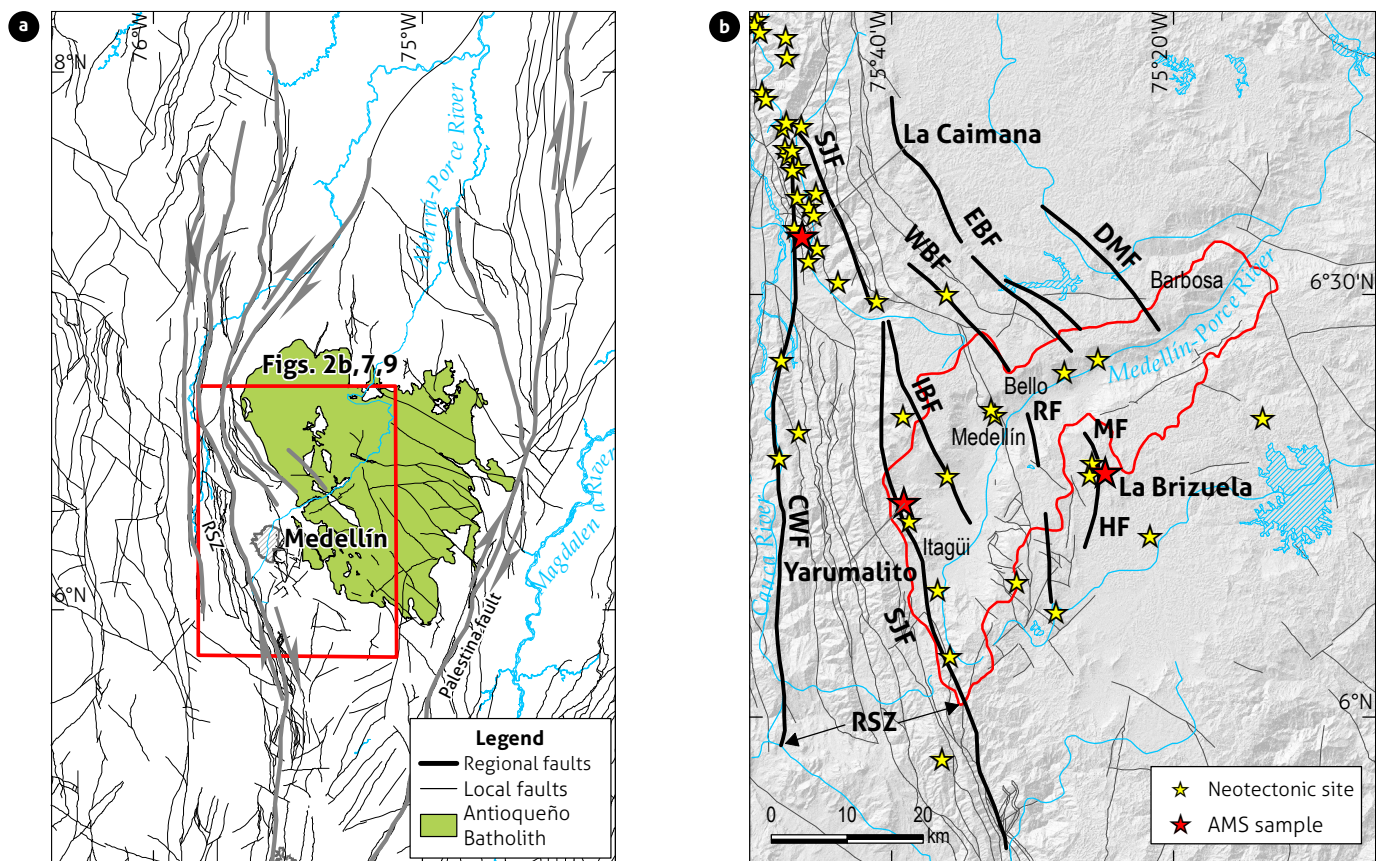
Figure 2. Detailed tectonic and geomorphic expression of the Central Cordillera controlling AV´s morphotectonic
a) Main tectonic boundaries in the Northwestern Andes (black lines) and location of the study site between the RSZ, and the Antioqueño Batholith which is shown as green polygon in the center of the Central Cordillera (Gómez-Tapias et al., 2015). b) Active faults in the surroundings of the AV, named as SJF = San Jerónimo Fault, CWF = Cauca West Fault, IBF = Iguaná-Boquerón Fault, WBF = Western Belmira Fault, EBF = Eastern Belmira Fault, RF = Rodas Fault, DMF = Don Matias Fault, MF = La Mosca Fault, and HF = La Honda Fault. Along these faults several neotectonic sites have been reported previously (see Table 1), and three of them were selected for AMS analysis.

ne a simplistic tectonic model for the AV (Arias, 1995; Rendón et al., 2006; Restrepo-Moreno et al., 2009). Faulted deposits in western, central and northeastern sites of the AV suggest that tectonic deformation is still active in the region (e.g., Rendón, 2003; Yokota and Ortiz, 2003).

Geophysical data provide clues to estimate the crustal structure of the AV, suggesting an average crustal thickness of ca. 50-55 km in the Antioqueño Batholith area (Henao Casas and Monsalve, 2017; Poveda, 2013). This value is higher than the average of 30-40 km for the North Andean block (Ojeda and Havskov, 2001). On the other hand, Rendón (2003), using a geoelectrical survey, demonstrated that basement rocks of the AV are deformed by RSZ-related faults configuring a complex system of pull-apart basins and pop-up structures, segmenting the erosional surfaces of the Central Cordillera, just in the transition to the Antioqueño Batholith.

The tectonic geomorphology of the AV is analyzed by Rendón (2003) as a landscape response to tectonic and climatic forcing. Then, Rendón et al. (2006) and Aristizábal and Yokota (2008) propose chronostratigraphic frameworks of slope and alluvial deposits between the Late Pliocene and Late Pleistocene based on fission tracks and radiocarbon ages. These works include the previous datasets from Restrepo (1991), Silva (1999), Toro (1999) and Toro et al. (2006), improving the AV models with the implementation of quantitative geomorphic analysis and dating techniques. Several swath profiles and longitudinal river profile analyses made by Aristizábal and Yokota (2008), and Rendón (2003) indicate the knickpoints and knickzone locations of the main river and some of its tributaries.

The main knickpoints coincide with geomorphic features controlled by faults such as north Ancón and south Ancón and deformed basins previously highlighted. Although some of the faults reported as crossing the AV show deformation over recent sediments, their ages and displacement rates remain undocumented (Table 1). Future efforts on neotectonic studies need to concentrate on dating faulted or deformed sediments to quantify the timing and rates of active faults and ultimately to expand the temporal window by exploring paleoseismological and even archeoseismological records.

RSZ historical earthquakes, and hence the AV's seismic history, are documented in the area (Espinosa, 2003), but the most recent events were concentrated in the southern part of the Romeral megastructure, such as the 5.5 Mw Popayan earthquake in 1983 (Lomnitz and Hashizume, 1985); 6.4 Mw Páez earthquake in 1994 (Wilches-Chaux, 2005); and 6.2 Mw Quindío earthquake in 1999 (Gallego et al., 2005). In the northern part, close to AV, Suter et al. (2011) indicates the occurrence of pre-Hispanic Holocene earthquakes, and Caballero (2014) highlights events reported in Medellín by historians during the 18th century.

3. Methodology

3.1. Identification and sampling of deformed sediments for AMS analysis

To constrain the tectonic imprints on recent deposits, we choose samples for AMS analysis from sites restricted to fault traces with a well-defined morphotectonic expression and previously documented Quaternary deformation (Table 1). We chose pla-

Table 1. Main features of active faults in the surroundings of the AV separating major tectonic basins

Structure	Geometry	Kinematic	Brief description	Deformed sediments	References
Romeral shear zone	N-S to NNW-SSE/ high angle to E	Predominantly inverse. Left-lateral North of 5° latitude and right-lateral to the south	Constitute the PDZ and include San Jerónimo and Romeral faults. Exhibit high geomorphic expression, control southwestern basins of Aburrá Valley	Displacement of Holocene clayed terraces in Santa Fe-Sopetrán depression, and Late Holocene alluvial deposits in Yarumalito school and Late Holocene paleosols in close to Palmitas	Toro et al. (1999), Ortiz (2002), Vinasco and Cordani (2012), Suter et al. (2011), Lalinde et al. (2009)
Belmira Fault	N-S to N30W	Inverse with left-lateral component	Control the Rio Chico catchment and show displaced deposits. It is related to Calles Fault to the east and El Carmen Fault in the transition to the west. Its southern trace connects with Don Matias Fault	Deformed Pleistocene mudflow	Integral (1982), Mejía (1984), SGM (2002), Rendón (2003), Álvarez and Trujillo (1989)
Don Matias Fault	N30-40W	Inverse with left-lateral component	Continuity of the Belmira fault to the southeastern	Deformed Pleistocene mudflow	Integral (1982), Rendón (2003)
Rodas Fault	N-S/subhorizontal	Inverse	Fault associated with Aburrá Ophiolitic complex emplacement in the eastern hillslopes of the valley		Rendón (2003)
La Honda Fault	N-S/50-75E	Inverse/left lateral (?)	Control the Honda creeks in the east erosion surface beside the AV.	Deformed Holocene volcanic ash layers and Pleistocene fluvio-lacustrine deposits	Integral (2000), SGM (2002), Rendón (2003)
La Mosca Fault	NNW/subvertical	Inverse/left lateral (?)	Control the La Mosca creeks in the east erosion surface beside the AV.	Displacement of Holocene volcanic ash layers and Plio-Pleistocene fluvio-lacustrine deposits close the La Mosca Creek	Pages and James (1981), Rendón et al. (2015)
La Iguaná-Boquerón Fault	N-S to N12-20W/ high angle to E	Unknown	Fault associated with the Romeral shear zone	Deformed Pleistocene mudflows	Ortiz (2002), Rendón (2003)

ces from the available neotectonic sites based on: i) deformed sediments of known age, and ii) fine grain size fractions (i.e., high contents of silt and clay) to improve sampling. Prior to the sampling phase, we made geomorphologic maps at 1:10 000 scale, combining the main fault traces and Quaternary deposit distribution, which allowed us to identify the structural and morphotectonic framework of each place. Additionally, stratigraphic relationships of the deformed sediments with the surroundings were described, as well as the measurement of geological structures such as fault planes that affect the selected outcrops. Then, we sampled deformed soft-sediment material, mainly silt to clay layers, using polystyrene boxes of 8 cc. Each box was marked and fully oriented in the field using a Brunton compass and following the AGICO (2011) protocol.

3.2. Magnetic fabric of deformed sediments

The AMS of sedimentary samples can be represented as a magnetic fabric ellipsoid shape defined by the geometric distribution of the magnetic susceptibility tensor ($k_1 \geq k_2 \geq k_3$ axis) of a set of minerals in a previously oriented sample. As the magnetic susceptibility (k) refers to the ability of the minerals to acquire induced magnetization (Bilardello, 2016; Borradaile, 1988), the magnetic fabric ellipsoid shape represents how paramagnetic (e.g., pyroxenes, amphibole, biotite, etc.) and magnetic minerals (e.g., magnetite, hematite, iron, etc.) distribute in space (Parés, 2015). The magnitude of magnetic fabric can be expressed by the degree of anisotropy ($P = k_1/k_3$) and the shape of the magnetic fabric ellipsoid is conveniently described by the shape parameter (Jelinek, 1981); $1 > T > 0$ reflects oblate or planar shapes whereas $-1 < T < 0$ reflects prolate or linear shapes (Jelinek, 1981).

In deformed environments, the textural and magnetic fabric of fine sediments is coaxial with the directions of the principal strain axes; in these cases, the AMS ellipsoid can be represented as a deformation ellipsoid (Levi et al., 2014; Parés, 2015; Parés and Pluijm, 2002). While undeformed sediments tend to show oblate shapes, during extension or compaction the AMS ellipsoid changes progressively to a prolate shapes. As the deformation continues ellipsoid shapes become oblate again showing higher degrees of anisotropy compared to in previous stages of deformation (Parés, 2015; Soto et al., 2009; Weil and Yonkee, 2009). In neotectonic analysis, magnetic foliation of samples located in active fault zones is valuable because addresses shear plane orientations while magnetic lineation (k_1) indicates the shear direction. Due to this, the AMS

approach becomes a valuable tool to measure and characterize the magnetic fabric of brittle faults and fault-deformed soft sediments (e.g., Borradaile and Henry, 1997; Casas-Sainz et al., 2018; Hamilton et al., 2004; Levi et al., 2014, 2018; Maffione et al., 2012; Soto et al., 2009).

A total of one hundred specimens were analyzed using the AGICO MFK1-FB Multifunction Kappabridge Magnetic susceptibility meter. Magnetic fabric data were acquired using Safyr4 W software (AGICO, 2011). Measurements were made at room temperature and under an operational frequency of 976 Hz and a low-intensity magnetic field of 200 Am^{-1} at the Paleomagnetism Laboratory of the Universidad EAFIT. Fifteen default positions for measurement were conducted according to the Jelinek protocol (Jelinek, 1977). After the Kappabridge measurements, we used the advanced treatment of magnetic anisotropy data - Anisoft software version 5.1.03 (Chadima and Jelinek, 2019), to produce the susceptibility mean tensor and its statistical error and to compute the AMS parameters and graphic results, such as the Jelinek (T-Pj), Flinn (L-F), and T-L diagrams.

3.3. Structural analysis

Theoretically, in a Riedel shear model, the principal displacement zone (PDZ) constitutes the general trend of the major shear zone which responds to a regional stress field (Cloos, 1928; Davis et al., 2000; Riedel, 1929). A synthesis of the geometric relationship of the basic structures and their sequential development in a stress field is presented by Cloos (1928), Busby and Bassett (2007), Cosgrove (2007), Gurbuz (2010), Mann et al. (1983), Noda (2013), Passchier and Trouw (2005), Ramsay (1980), Riedel (1929), Traforti et al. (2016), among others. In this model, the synthetic Riedel fault (R) is the first to be developed at angles of ca. 30° with respect to the maximum stress vector (σ_1). Progressively, a second structure, the antithetic Riedel fault (R'), appears with the same angle on the opposite side of the maximum stress vector plane (σ_1), showing conjugate shear deformation. As deformation evolves, P and P' shears appear as minor faults located symmetrically at ~55° to the main compressional vector (σ_1). The Y shears are minor synthetic faults parallel to the PDZ, and T represents tension fractures parallel to the maximum stress vector plane (σ_1).

A tectonic framework of the AV was reviewed and analyzed from theoretical models of deformation in strike-slip environments and available literature of the study site. For the first part, we applied the Riedel shear model (Riedel, 1929) to geome-
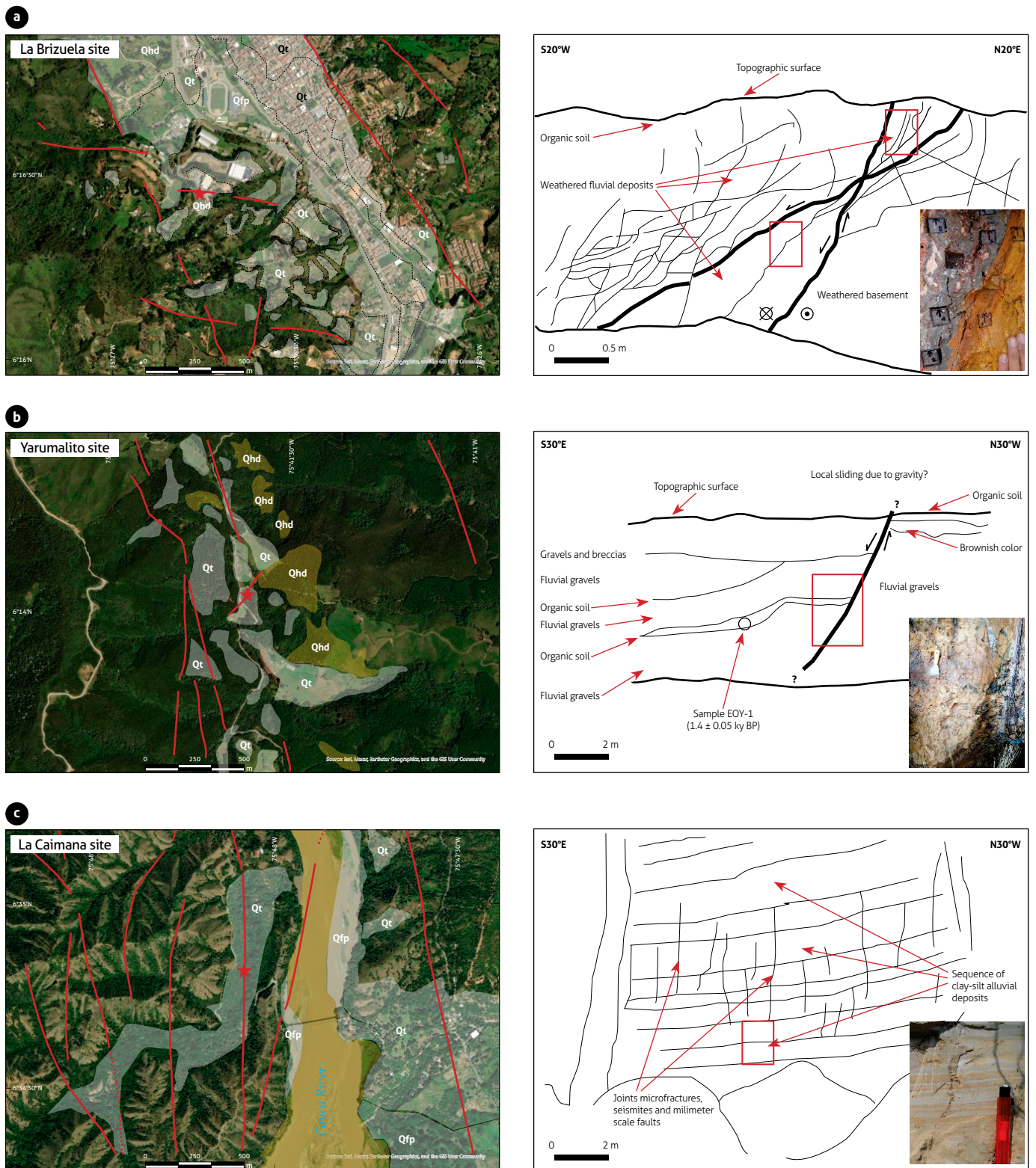
Figure 3. Selected sites for AMS analysis
a) Faulted Pleistocene (?) alluvial deposit along the La Mosca satellite Fault at the La Brizuela site. b) Faulted Holocene soil along the San Jerónimo Fault at the Yarumalito site. c) Apparently undeformed Holocene deposits covering the Cauca West Fault close to Santa Fe de Antioquia town. Red stars mark the specific location of the AMS analysis while red lines are the local faults covered by Quaternary deposits (Qt = Terrace, Qfp = Flood plain, Qhd = Hillslope deposit)

trically define the PDZ and hence estimate the kinematics of faulting and to identify neotectonic patterns in the AV that can be described by strike-slip faulting. In this stress-strain conceptual model, a hierarchy of structures can appear as the deformation evolves through time (Busby and Bassett, 2007; Mann et al., 1983; Noda, 2013). Then, we reviewed and compiled the geometry and kinematics of regional faults with neotectonic activity reported in the literature (Table 1). These faults were delineated using their geomorphic expression in a digital elevation model (DEM) with a 12.5 m spatial resolution. The DEM was downloaded from https://www.asf.alaska.edu, and the Topo toolbox v 2.2 (Schwanghart and Scherler, 2014) was used for longitudinal river profile extraction and knickpoint identification. In the field, mesoscale faults and structural datasets observed at the selected sites for AMS analysis were measured and compared with the magnetic fabric of deformed soft sediments. As the structural data provide the geometry of the fault plane, the AMS was used to evaluate the sense of motion of the structure. Finally, these data were compared with fault architecture derived proposed models of tectonic evolution of the AV.

4. Results

4.1. Neotectonic sites and deformed sediments
The three selected sites with occurrence of Quaternary fluvio-lacustrine deposits and imprinted deformation of active faults are shown in Figures 2 and 3. They correspond to the La Brizuela (Guarne), Yarumalito (San Antonio de Prado), and La Caimana (Santa Fe de Antioquia) sites. Table 2 describe

main geologic features of each site. While the first one represents active faulting on the eastern side of the AV, the last two correspond to active faulting along the RSZ. Surface ruptures and faulted/buried sediments are characteristic at La Brizuela and Yarumalito sites, as opposed to the La Caimana site, where horizontal layers of apparently undeformed sediments cover active faults of the Cauca River Canyon. Gray-clayed sediments of the La Brizuela site exhibit inverse relief and high weathering grades, with estimated Plio-Pleistocene ages (Page and James, 1981) and deformation related to the La Mosca fault (Rendón et al., 2015). A total of 55 samples were collected at this site, with 12 samples distributed in the footwall block, 23 in the hanging wall block beside the principal fault plane, and 20 samples from apparently undeformed sediments (Figure 3a). Along the RSZ, the Yarumalito and La Caimana sites correspond to Holocene alluvial deposits (Yokota and Ortiz, 2003; García et al., 2011) covering the San Jérónimo and Cauca West faults respectively (Figures 3b and 3c). At the Yarumalito site, we collected 9 samples from the footwall and 6 from the hanging wall for a total of 15 samples. Finally, 30 samples of horizontally layered nondeformed sediments were collected at the La Caimana site.

4.2. AMS measurements of deformed sediments
The results of the AMS measurements are shown in Table 3. The shape parameters of the magnetic fabric ellipsoid are summarized in Figure 4. The mean susceptibility (k_m) versus corrected anisotropy shape factor (P_j) and the Jelinek diagram (Pj-T) are shown in Figure 5.

Table 2. Main geologic features of the selected sites for magnetic fabric analysis

Site	Structural features	Stratigraphic/ geomorphologic features	References
La Brizuela	Main structure: La Mosca Fault. Geometry: NNW/subvertical. Kinematic: Inverse/left lateral (?). Associated structures: normal faults at N85W strike. Marks the structural boundary between the Antioqueño Batholith to the east and the eastern structures of the RSZ controlling the landscape along La Mosca Creek.	Surficial formations: Alluvial terraces of the La Mosca Creek and associated slope deposits. Estimated age of deposits covering the fault: Pliocene to Pleistocene age for high elevated terraces showing high weathering grades (Bauxite). Type of deformation: Centimetric deformation along a mayor plane of displacement affecting highly weathered alluvial deposits.	Pages and James (1981); Rendón et al. (2015)
Yarumalito	Main structure: San Jérónimo Fault (RSZ). Geometry: N-S to NNW-SSE/high angle to E. Kinematic: Predominantly inverse Left-lateral North of 5° Latitude and right-lateral to the south. Associated structures: Satellite fault at 185/75 with normal movement.	Surficial formations: Alluvial deposits covered by relatively young paleosol. Estimated age of deposits covering the fault: Radiocarbon age of ca. 1400 y BP from paleosol. Type of deformation: Normal fault displaces alluvial deposits and paleosol at the Yarumalito school (San Antonio de Prado) affected by a satellite fault of the San Jérónimo Fault.	Ortiz (2002), Yokota and Ortiz (2003), Lalinde et al. (2009)
La Caimana	Main structure: Cauca West Fault (RSZ). Geometry: N10°W. Kinematic: Unknown, inferred as lateral left. There are positive flowers at mesoscale close to Santa Fe de Antioquia. Associated structures: Cauca West subparallel anastomosed faults.	Surficial formations: Alluvial and lacustrine deposits developed as consequence of Cauca´s River natural damming. Estimated age of deposits covering the fault: Late Holocene radiocarbon ages from 0.1-6 ky. Type of deformation: soft sediment displacement and seismites with locally undeformed outcrop.	Suter et al. (2011); García et al. (2011)

Table 3. Group statistics of the anisotropy of magnetic susceptibility (AMS) from the deformed sediment samples in the surroundings of the AV

Site	Sample	N	k_m	sdv	k1		k2		k3		L	sdv	F	sdv	P_j	sdv	T	sdv
					Decl.	Incl.	Decl.	Incl.	Decl.	Incl.								
La Brizuela	All deformed samples	35	75.3	77.9	221.4	19.4	77.2	66.5	315.9	12.7	1.055	0.059	1.072	0.105	1.138	0.156	0.126	0.394
	Footwall	12	140.8	102.1	233.6	2.3	136.8	71.3	324.4	18.6	1.087	0.074	1.064	0.052	1.162	0.125	0.087	0.464
	Hanging wall	23	43.58	32.88	204.7	46.7	30.5	43.1	297.8	2.9	1.035	0.032	1.074	0.125	1.120	0.168	0.192	0.360
	Non-deformed samples	20	45.21	48.12	181.8	40.4	10.5	49.3	275.0	4.3	1.014	0.011	1.025	0.034	1.041	0.042	0.048	0.431
Yarumalito	All samples	15	450.5	202.9	38.1	71.4	219.2	18.6	129.1	0.3	1.006	0.003	1.008	0.004	1.014	0.004	0.094	0.427
	Footwall	6	491.7	253.5	52.0	68.2	254.2	20.3	161.4	7.5	1.006	0.002	1.007	0.005	1.013	0.003	0.075	0.575
	Hanging wall	9	422.9	172.4	27.7	70.7	181.8	17.5	274.3	7.9	1.006	0.002	1.008	0.004	1.015	0.005	0.107	0.333
La Caimana	Non-deformed samples	30	708.7	139.5	114.2	85.8	308.1	4.0	218.0	1.0	1.008	0.004	1.027	0.005	1.037	0.007	0.533	0.163

Notes: N = Number of analyzed samples, k_m = mean susceptibility (in 10^{-6} SI units), (Decl) Declination and (Incl) inclination of the three-susceptibility axis (geographic coordinates), L = Lineation, F = Foliation, P_j = Corrected anisotropy degree, T = Shape factor of the AMS ellipsoid.

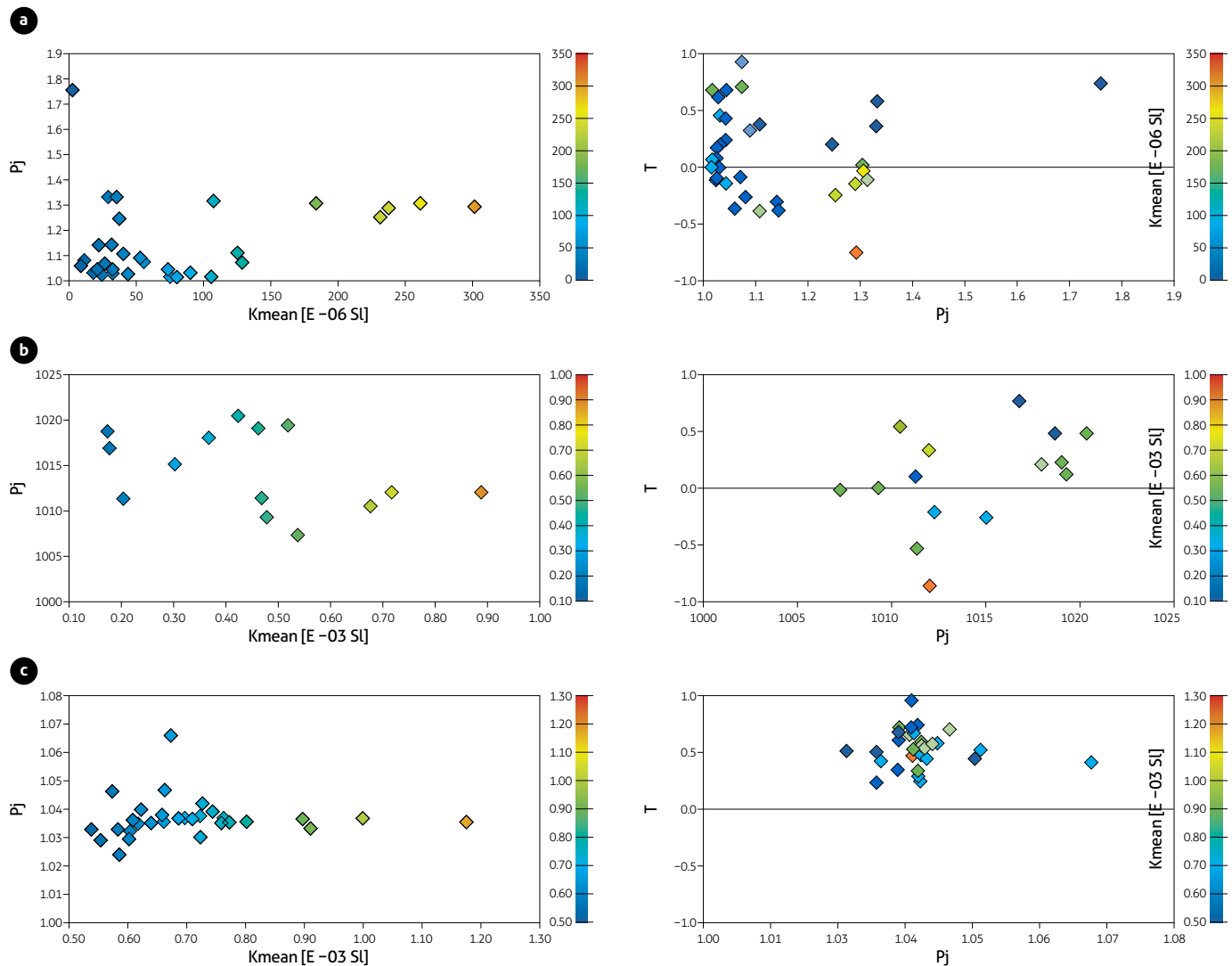**Figure 4.** Magnetic fabrics of deformed sediments at the sites: a) La Brizuela, b) Yarumalito, and c) La Caimana

Figure 5. Mean susceptibility vs Corrected anisotropy shape factor and Jelinek diagram (Pj-T) of the deformed deposits at a) La Brizuela, b) Yarumalito, and c) La Caimana

The magnitude of the mean susceptibility ranges between 0 and $300*10^{-6}$ SI, with average values of ca. $75.31*10^{-6}$ SI at the La Brizuela site. At the Yarumalito site, the average susceptibility is $450.5*10^{-6}$ SI, with values ranging between 150 and $900*10^{-6}$ SI. The mean susceptibility values of La Caimana range between 500 and $1200*10^{-6}$ SI, with an average of $708.7*10^{-6}$ SI. In all cases, the k_m values were on the order of 10^{-3} SI, except for the La Brizuela results, where k_m reached values near 10^{-6} SI. The Jelinek diagram indicates that samples from La Brizuela and Yarumalito exhibit mixed prolate and oblate ellipsoid shapes with P_j values of less than 1.8, while samples from La Caimana show well grouped oblate ellipsoids with P_j values

between 1.02 and 1.07 (Figure 5). The F-L and L-T diagrams (Figure 6) show the well-defined triaxial ellipsoids of the Yarumalito and La Brizuela sites despite the large dispersion of this last sample. For the La Caimana samples, the results indicate oblate ellipsoid shapes.

4.3. Structural models and magnetic fabric data

As the AV is located between the Antioqueño Batholith and the RSZ, its tectonic history needs to be a consequence of the evolution of these major geomorphic features. For our structural analysis, we define the RSZ, with a main strike of ca. N20°W, as the PDZ controls the major shear zone, which responds to the
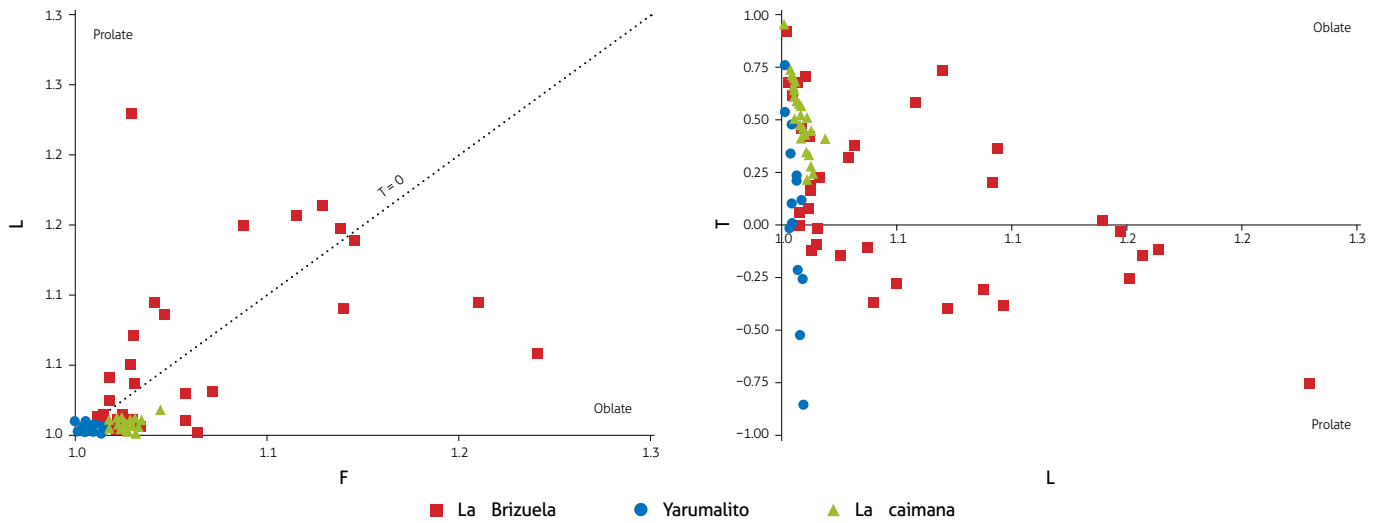
Figure 6. Shape parameters of the magnetic fabric ellipsoid and Flinn diagram for samples located in La Brizuela, Yarumalito, and La Caimana

regional stress field (Riedel, 1929; Ramsay, 1980; Davis et al., 2000). Then, assuming a left-lateral displacement of the PDZ (Gallego, 2018; Paris et al., 2000), our analysis indicates the occurrence of synthetic faults (R) with NNW strikes and left-lateral displacement along the RSZ and Antioqueño Batholith transition (Figures 2 and 7). These structures extend across the basement of the AV forming gorges (i.e., Ancones) and tectonic valleys, and exhibit their expression along the longitudinal river profile of the Medellín-Porce River as knickzones (Figure 8). Based on the spatial distribution of these faults, and tectonic/geomorphologic models proposed by Rendón (2003) and Aristizábal and Yokota (2008), we separate the AV valley into four main sections (or subbasins) named Itagüí, Medellín, Bello and Barbosa, from South to North.

The first and uppermost section includes the Itagüí tectonic subbasin with irregular depths varying between ca. 75 m to ca. 220 m, the Altavista Stock and the older and highly deformed deposits of the AV located in La Tablaza, Caldas (Rendón et al., 2006; Toro et al., 2006). This southwestern portion of the AV is directly influenced by the San Jerónimo Fault as the latter controls the Doña Maria creek and the headwaters of the Medellín River (Rendón et al., 2006) (Figures 2, 7 and 8). Highly dense anastomosed geometry of faults with fault bending basins (R-start displacement) appear dominating the landscape in this section of the AV.

The second section corresponds to the Medellín tectonic subbasin, located on the western-central side of the AV. In this sec-

tion, the AV exhibits a major width of ca. 10 k, following a NW trend narrow depression of ca. 240 m depth that appears related to the Boquerón-Iguaná Fault trace Rendón (2003) (Figure 7). Topographic highs located in erosion surfaces on both sides of the AV such as the Baldías (~3200 masl) and Santa Elena (~2600 masl) are included in this segment. Step-over basin geometries were identified in this section with the dominance of NW to EW striking normal faults (coaxial with antithetic R´ structures).

A third section of the AV includes the Bello tectonic subbasin with less than 110 m depth and the Ovejas Stock delimited by the western Belmira Fault. This section acts as a transition to the Antioqueño Batholith domain, as well as inherited structures associated with Aburrá´s ophiolitic complex (Ibáñez-Mejía et al., 2020). This section also exhibits fault-terminated basins with WNW normal faults (Rendón, 2003).

The fourth section is on the northeastern side of the AV and inside the granodiorite body of the Antioqueño Batholith. This section exhibits a completely different landscape and tectonic regime in terms of valley morphology following a well-defined NE trending V-valley shape separating the extensive erosion surfaces of the AP and vertical elevation differences of ca. 1 km. The occurrence of tectonic controls of NE strikes in this section of the AV can be related to P´ structures. As a synthesis, the AV can be understood as a complex coalescence of tectonic basins located in the middle and upper sections of the AV. They appear as lazy-S shaped basins (Mann et al., 1983) immediately beside the RSZ (i.e., Caldas, La Estrella and
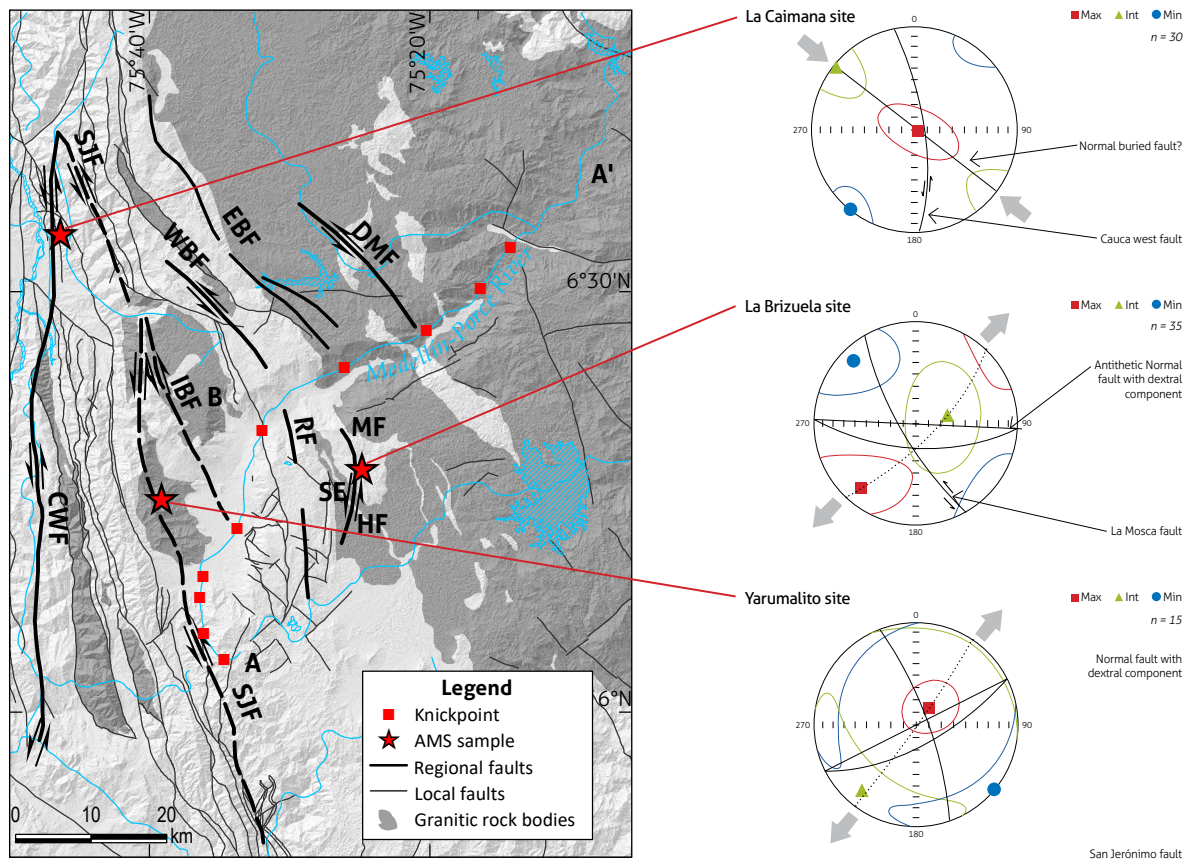
Figure 7. Comparison of magnetic fabric ellipsoid and structural datasets of active faults at La Caimana, La Brizuela, and Yarumalito sites, and a synthesis of the Riedel shear model indicating the occurrence of primary and secondary structures under a known strain field
Longitudinal river profile is marked from A to A'. SJF = San Jerónimo Fault, CWF = Cauca West Fault, IBF = Iguaná-Boquerón Fault, WBF = Western Belmira Fault, EBF = Eastern Belmira Fault, RF = Rodas Fault, DMF = Don Matias Fault, MF = La Mosca Fault, and HF = La Honda Fault. B = Baldías, SE = Santa Elena.
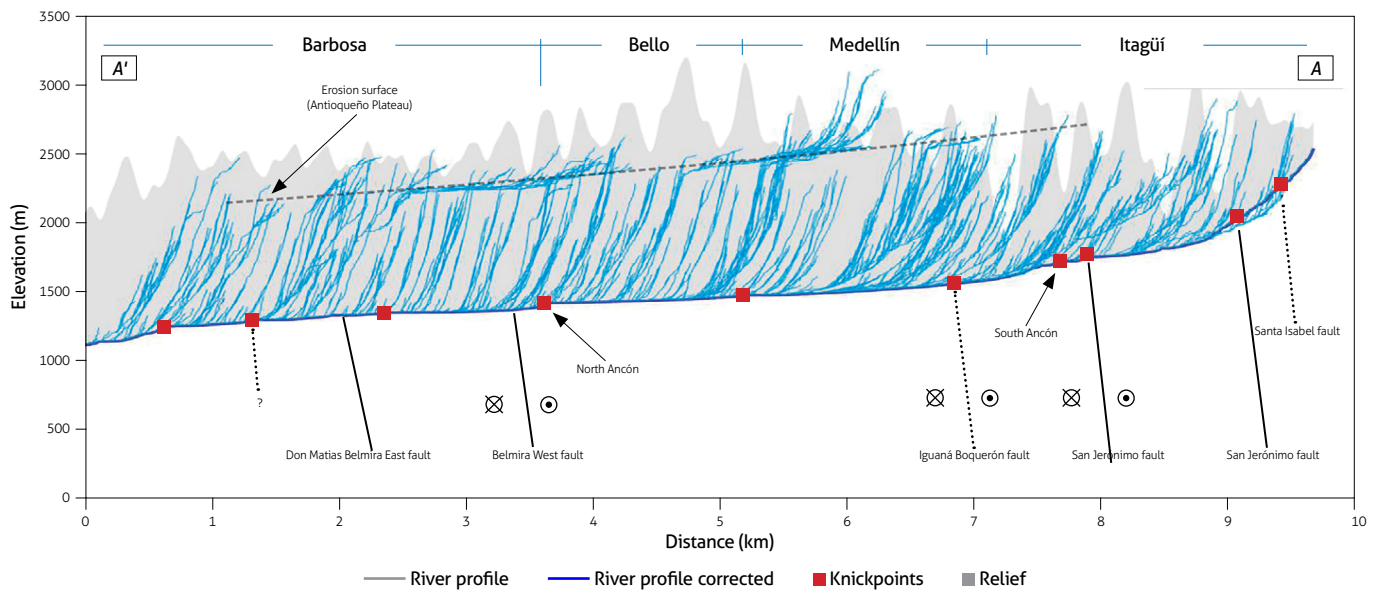
Figure 8. Longitudinal profile of the Medellín Porce River indicating the spatial distribution for the four tectonic basins of the AV separated by local faults (Rendón, 2003)

San Antonio de Prado) comprising the upper AV. In the middle portion of the valley, tectonic basins appear as releasing bend step-over and/or rhomboidal shaped pull-apart basins (i.e., Bello and Medellín subbasins) (Figure 7).

The structural and magnetic fabric data obtained at the outcrop scale are presented in Table 4. In addition, Figure 7 shows the principal directions of the AMS ellipsoid integrated with the geometry and kinematics of the measured fault planes at the three selected sites for detailed analysis.

Although the La Mosca fault has a general strike of ca. N30°W, subvertical dip and left-lateral displacement, our structural data from the La Brizuela site indicate normal faulting along the 185/75 plane. The magnetic fabric ellipsoid shape shows mean values of declination/inclination of 221.4/19.4 for k_{max} and 345.9/12.7 for k_{min}. Slight differences were found between samples from both sides of the La Mosca fault, as the k_{max} magnetic lineations were ~204.7/46.7 for the hanging wall, and ~233.6/2.3 for the footwall. The results from apparently nondeformed sediments also show magnetic lineation of 181.8/40.4. In the fault zone, mixed ellipsoids between oblate and prolate shapes suggest high magnetic foliation toward the south and southeast and magnetic lineation indicating normal displacement with a dextral component along the WNW fault plane.

At the Yarumalito site, a mixed prolate-oblate ellipsoid with marked magnetic foliation ranging between 94/82 and 162/83, subparallel to the 150/70 fault plane, and subvertical lineation indicate predominantly normal faulting with a dextral component. Buried faults in the La Caimana site follow the regional trend of the RSZ (i.e., NS to NNW), although our AMS ellipsoid indicates a subvertical magnetic cleavage of 114.2/85.8 (Figure 7).

5. Discussion

Deformed sediments are critical in active tectonic settings because they record the timing and magnitude of ancient earthquakes and provide clues for detailed palaeoseismological analysis (McCalpin, 2012). Our data provide new clues to understanding the neotectonic framework of the AV and its surroundings as well as a practical approach to tectonic geomorphology, structural geology, and AMS analysis in seismic hazard studies. Previous geophysical data indicate faults controlling AV's topographic structure and sedimentary infill (Rendón, 2003; Henao Casas and Monsalve, 2017). These structures exhibit marked geomorphic expressions along each tectonic subbasin and the whole drainage network and deform Quaternary deposits in some parts of their main traces (see Table 1).

Because the structural data from deformed sediments yield the geometry of the fault plane, the AMS provides clues on the kinematic of the fault , and k_{max} tends to align in response to the stress field, we used the obtained magnetic lineation (k_1) as a shear direction indicator in neotectonic studies (Caricchi et al., 2016; Cho et al., 2014; Levi et al., 2014; Parés and Pluijm, 2002). In this study, all the collected samples show deformational magnetic fabric, i.e., subhorizontal k_{min} distribution even on apparently nondeformed samples of La Caimana and La Brizuela (Figure 4). The occurrence of magnetic fabric on evidently nondeformed sediments is also documented by Cifelli et al. (2004) indicating the development of a stress field during the incipient deformational phase. In addition, the obtained mean susceptibility (k_m) values were on the order of 10^{-3} SI, except for the La Brizuela results, where k_m reached values in the range of 10^{-6} SI (Figure 5) suggesting that the net contri-

Table 4. Summary of the magnetic fabric and structural dataset from the analyzed sites

Fault	Site	Sample	n	AMS ellipsoid shape	Magnetic lineation (k_{max})	Magnetic foliation	Magnetic fabric	Structural data
La Mosca	La Brizuela	All deformed samples	35	Triaxial oblate to elongate	221.4/19.4	136/76 (NE-SW)	Compressional/cleavage development	Fault plane: 185/85, 183/73, 180/74
		Footwall	12	Triaxial oblate	233.6/2.3	144/71 (N50E-S50W)	Compressional/cleavage development	
		Hanging wall	23	Triaxial	204.7/46.7	118/87 (NE-S28W)	Compressional/cleavage development	
		Nondeformed samples	20	Triaxial	181.8/40.4	95/85 (N05E-S05W)	Shear-related/deformational fabric	
San Jerónimo	Yarumalito	All samples	15	Triaxial	38.1/71.4	129/89 (N39E-S39W)	Shear-related/deformational fabric	Fault plane: 150/70
		Footwall	6	Triaxial	52.0/68.2	162/83 (N72E)	Shear-related/deformational fabric	
		Hanging wall	9	Triaxial	27.7/70.7	94/82 (N04E)	Shear-related/deformational fabric	
Cauca West	La Caimana	Nondeformed samples	30	Triaxial oblate	114,2/85,8	308/89 (N52W)	Shear-related/deformational fabric	Horizontal bedding plane. Fault plane (covered): 90/90, 270/85

bution of ferromagnetic minerals to the susceptibility and to the AMS is not considerable (Parés, 2015). Large differences in mean susceptibility for the three sampling sites may reflect some postdepositional or tectonically induced changes in magnetic mineralogy, as well as the potential effect of weathering in the older deposits of La Brizuela. In general, the AMS ellipsoids from the La Brizuela and Yarumalito sites correspond to a slightly similar extensional deformation following a NE-SW orientation, while the AMS ellipsoid from the La Caimana site shows a highly compressional/rotational system with a NW strike for the major plane (Figure 6).

Also, the AV comprises a complex valley after the coalescence of multiple tectonic subbasins in the transition zone between the AP and the RSZ morphotectonic domains. For a better understanding of the tectonic history of the AV, we discuss the structural and magnetic results for two main sections that include our AMS sites, the AV to AP transition zone under a high contrast of basement anisotropies, and the RSZ, where the PDZ marks the main trend of deformation along the study site.

5.1. AV-AP transition zone

The la Mosca fault (LMF) is an approximately N10°W, inverse and left lateral, high dip fault located on the eastern side of the AV (Figure 7). Its trace controls La Mosca Creek, which crosses Guarne town. Gallego (2015) indicates that the La Mosca and La Honda Faults coincide with a faulted contact between metamorphic basement and the Antioqueño Batholith. In geomorphologic terms, the La Mosca fault separates erosion surfaces and erosive scarps, as Rendón (2003) reported its correlation following the Eastern Belmira Fault (i.e., NW of AV). These structures represent the transitional expression of the strain partitioning on the farthest portion of the RSZ (i.e., Bello and Barbosa tectonic subbasins) but also seem to respond to the same regional strain field. Additionally, the northeastern part of the Medellín tectonic subbasin exhibits a fault-terminated basins with a Z-shape and basement of less than 110 m depth and a NW-SE trend (Figure 9).

At the la Brizuela site, AMS results show that the magnetic lineation of samples from the La Mosca Fault at the La Brizuela site indicates values of 205/47 to 234/03 (SW) and shear planes with poles ranging between 298/03 and 324/19 (NW). In contrast, the results from apparently undeformed samples located approximately five meters away from the fault trace (WNW) show magnetic foliation planes with a N-S trend (k_3 ~276/04) and magnetic lineation of ca. 180/40. The orientation of the

main normal plane shows a dextral component of displacement related to the development of antithetic faults (R´) which segment the principal trace of N10°W strike (Figure 7). This transitional section toward the AP was considered to represent relatively low neotectonic activity before the studies of Rendón et al. (2015), which showed continuous deformation along the La Mosca and La Honda Faults displacing alluvial deposits and volcanic ash layers.

AMS data from some of the alluvial deformed Quaternary deposits in the LMF support the fact of undocumented neotectonic features which creates the idea of relatively low tectonic and seismic activity but also updates the earthquake geology on the eastern side of the AV and its surroundings. This situation is caused in part due to the difficulties to find Quaternary deposits preserving fault displacements and deformation history of the region. Although that, recent studies have been updated the seismic hazard assessment in the region as new stratigraphic evidence have been documented.

Note that the structural analysis shown in Figure 9 marks the occurrence of NE structures corresponding to antithetic faults (P´) which control the northern section of the AV along the low anisotropy regime of the Antioqueño Batholith, while the antithetic faults (R´) cross the valley. Despite the lack of paleoseismological data from the LMF, neotectonic elements of this site mark a substantial active tectonics along a relatively low mechanical anisotropy (i.e., granitic and thermal metamorphic rocks). Note that fault-bonded granitic rock units such as Altavista and Ovejas stocks can be interpreted as segmented and transported blocks along the RSZ-related faults in its eastern side, indicating a progressive reduction in size as they approaches the main strain zone (i.e., the PDZ). Growing urbanism and concomitant modification make it difficult to document of detailed stratigraphic evidence of ancient earthquakes.

5.2. Romeral shear zone (RSZ)

The San Jerónimo and West Cauca faults constitute the eastern and outermost faults of the RSZ, displaying mainly NNW strike deformation. The morphological expression of fault traces and their associated morphotectonic features are well documented along this shear zone (Lalinde et al., 2009; Ortiz, 2002; Rendón, 2003). In addition, Late Holocene displacements of these faults (Yokota and Ortiz, 2003) allow us to propose and evaluate the hypothesis of this region as the PDZ.
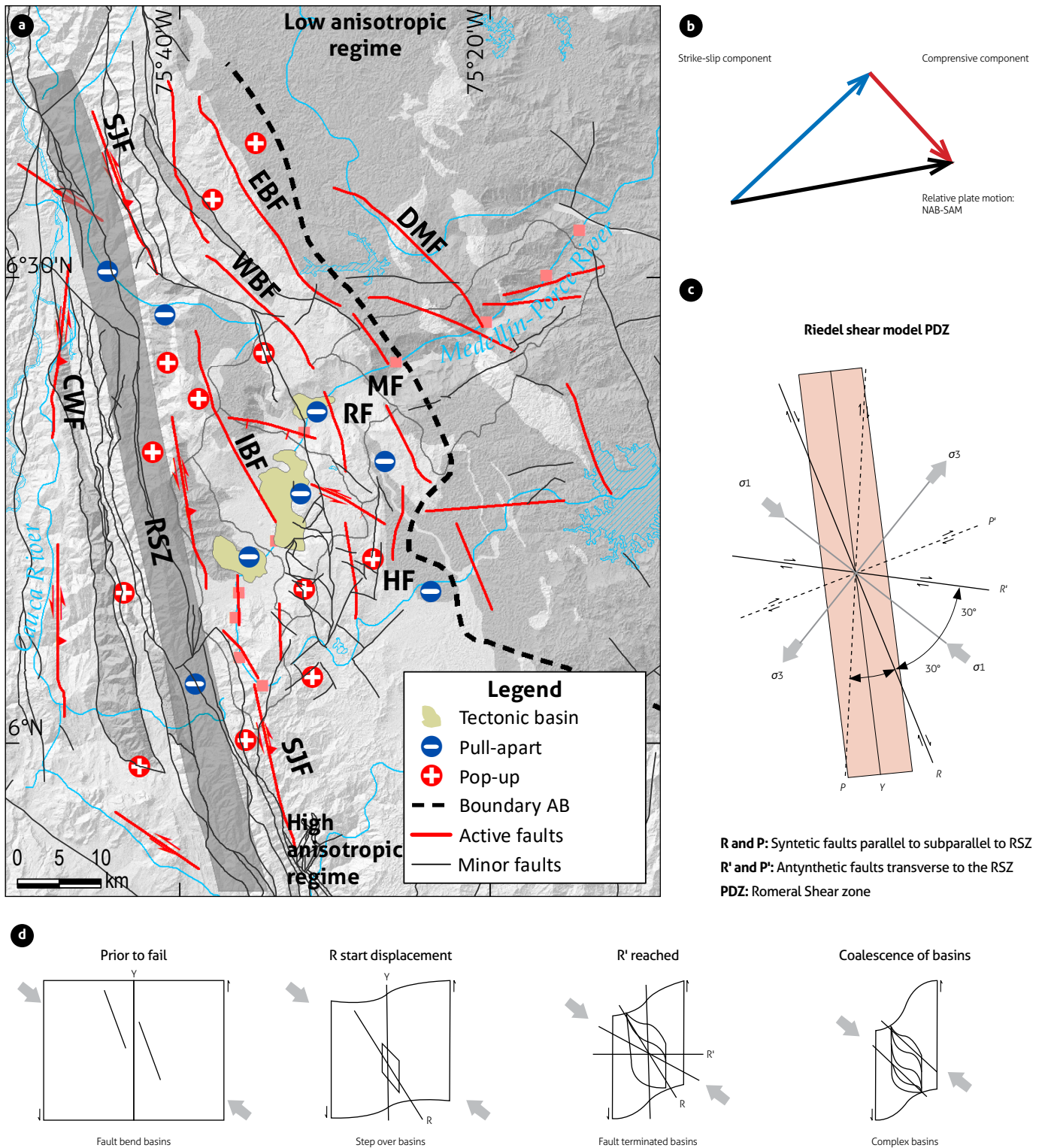
Figure 9. Conceptual model for a neotectonic framework of the AV

a) Crustal deformation models under strike-slip fault systems; b) Components of the relative plate motion between the North Andean Block (NAB) and the South America Plate (SAM). GPS vectors from Mora-Páez et al. (2020) and Noquet et al. (2014), in Kirby (2016); c) Simplified Riedel shear model under the present-day stress field and the compressive component. d) Simplified model of the evolution of coalescence transtensional/transgressive sedimentary basins (Mann et al., 1987; Noda, 2013).

The structural architecture in the Yarumalito site is defined by relatively more active faults that developed into step-over basins such as the upper Doña Maria catchment and the Medellín River headwaters, all of them in the Itagüí tectonic subbasin (Figure 9). Furthermore, a normal 150/70 satellite fault of the San Jerónimo Fault exhibits a more recent displacement (ca. 1.5 ky, from ^{14}C, Yokota and Ortiz, 2003), with a similar geometry and kinematics as found in the LMF, except for a different subvertical magnetic lineation of 94/82 and 162/83 (Figure 7). This expression of the magnetic fabric in the Yarumalito site marks an important horizontal component of displacement of faults in this section, where the anisotropic regime is considerably higher in comparison with the eastern section.

On the other hand, tectonic and magnetic results on the western side of the RSZ, i.e., the La Caimana site, contrast with previous sites (Figure 7). Late Holocene fine-grained sedimentary sequences overlying the Cauca West Fault (Suter et al., 2011) do not exhibit remarkable deformation at the local scale, and the more remarkable deformation shows millimetric displacement of silt layers. Triaxial oblate magnetic ellipsoid shapes, with a magnetic lineation of 114.2/85.8 and magnetic foliation plane of 308/89 (N52W), define a shear-related/deformational fabric of the La Caimana site consequent with a previous tectonic hypothesis of strike-slip faulting controlling the Santa Fe-Sopetrán depression along a section dominated by the Cauca River Canyon and RSZ. The obtained structural and magnetic dataset marks the RSZ as a PDZ of the neotectonic model of the AV. Additionally, these results on the western section of the RSZ are in agreement with the development of NW structures in a similar structural regime along the WC, including faults such as the Cañasgordas, Abriaquí, and Arma, among others (Paris et al., 2000; Noriega and Caballero, 2015; add more refs), all of which show a left-strike kinematics and Quaternary displacements.

5.3. Neotectonic and recent deformation in the surroundings of the AV

Based on the compiled and measured structural data of the active faults and associated structures in the study zone, we propose an interpretation of the brittle structures along the AV and their relationship with the surrounding first order geomorphic structures, such as the Antioqueño Batholith and the RSZ. Additionally, we propose that fault bending basins controlled by synthetic faults (R) appear in the early stages of deformation.

This is what we observed in the core of the PDZ (i.e., Itagüí subbasin) as corresponding to the more active and rejuvenated structure (Figure 9). As deformation continues, antithetic faults (R´) control the development of step-over basins with extended areas and deeper depocenters (Medellín and Bello subbasins). The long-term evolution of tectonic valleys creates complexes of coalescent valleys subbasins with overimprented tectonic and erosive processes (e.g., Mann et al., 1983; Noda, 2013). In our specific case, the PDZ was defined by the RSZ, as it represents the major structure controlling the strain partition in the study site. In addition, compressional vectors estimated from the deformational magnetic ellipsoid are coherent with geodesic vectors from Mora-Páez et al. (2020), as both indicate a NW-SE orientation of the maximum compressional component (σ_1), and they are consequent with the neotectonic framework of the Northern Andes (Costa et al., 2020).

Deformation in an oblique convergence tectonic setting produces strain partitioning, and hence faulting and folding, by transpression and transtensional mechanisms (Cosgrove, 2007; Ramsay, 1980). This setting is dominated by strike-slip regional faults that introduce crustal-scale heterogeneities. In this study, we assume that the massive granitic body of the Antioqueño Batholith has a different mechanical response than the surrounding fault-controlled lithologies included in the transition to the RSZ. This simplified scheme of differential mechanical response as a function of inherited anisotropy and rheology of the involved materials is coherent with the development and reactivation of faults controlling isolated tectonic basins conforming to the actual drainage system of the AV. Morphologic expression of their discontinuities appears along active faults separating tectonic basins and along the longitudinal river profile where some of them show knickpoint retreatment just upward of the main trace of the AV´s transversal faults.

In the AV, brittle deformation is produced by transpresive and transtensive displacement along strike-slip structures. Along this transition between the AB and the RSZ, these faults have produced a positive relief in the form of 'pop-up' topography and negative relief in the form of tectonic basins discussed and simplified in Figure 9. As the deformation concentrates and landscape evolves, complex structures of pull-apart basins appear (see Kim and Sanderson, 2006), with the subsequent filling of basins by sediments and the reorganization of the drainage network inside tectonic valleys since the Pliocene (Aristizábal et al., 2004; Rendón et al., 2006). Additionally, higher depocenters in the Medellín and Itagüí basins correlate with

the chronostratigraphic records documented in the AV (e.g., Rendón et al., 2006; García, 2006). In evolved stages of deformation during the Quaternary, isolated tectonic subbasins could combine by means of uplift processes, rising advance of the erosion wavefronts along the Medellín-Porce River, and the coalescence of subbasins, forming broader and more complex sedimentary basins (Mann et al., 1983; Noda 2013, etc.). This last event of landscape rejuvenation corresponds to the Pleistocene pulses of Andean Orogeny and hence the actual neotectonic regime that controls seismogenic sources in the AV and their surroundings.

6. Conclusions

The results and interpretation of the magnetic fabric and structural datasets previously presented allow us to conclude that:

» All the AMS data from selected neotectonic sites exhibit triaxial ellipsoids with k_{min} values distributed in a subhorizontal plane and subvertical k_{max} that define shear-related fabric and/or cleavage development. This implies that deformed and apparently undeformed sediments covering active faults record a magnetic fabric associated with the tectonic imprints of recent displacement, and it can be used as a strain indicators in further neotectonic studies.

» Magnetic and structural data from the La Brizuela site indicate normal faulting with a dextral component along an antithetic (R´) 185/85 plane with respect to the PDZ (~80/90). At this site, the magnetic lineation from Pleistocene alluvial deposits deformed by the La Mosca Fault variesbetween 182/40 and 234/03. A similar trend is obtained in the Yarumalito site with an antithetic (P´) 150/70 plane and normal displacement of the Late Holocene paleosol. At this site, the magnetic lineation of ca. 38/70 marks a dextral component.

» At the La Caimama site, apparently nondeformed sediments of Middle to Holocene ages covering regional faults such as the Cauca West; in the western section of the RSZ, they exhibit shear-related AMS ellipsoids with subvertical magnetic lineation of 114/85 and defining a 308/89 plane.

» Disparities between the kinematics of active faults in the study site are related to local responses of the regional strain field conditioned by lithology and inherited mechanical anisotropy overprinted on recent markers of deformation such as Quaternary deposits.

» The presented results show that Quaternary sedimentary deposits affected by active tectonic processes preserve the shape of the magnetic fabric ellipsoid, which is associated with the fault-plane solutions at the La Mosca, San Jerónimo and Cauca West faults. This work demonstrates the feasibility of the AMS analysis application to the characterization of active faults and neotectonic studies, and it advances a methodological approach that allows the production of data relative to past earthquakes and seismic hazards in the surroundings of the AV.

References

AGICO. (2011). *User Manual SAFYR4W* (p. 45).

Álvarez, C., Trujillo, R., & Hermelin, M. (1984). Aspectos geomorfológicos y estructurales del valle del norte de Aburrá. *1st Confecence on Geological Hazards in the Aburrá Valley*, 1-12.

Arbeláez, C. (2019). *Contribuciones desde la geomorfometría y la geomorfología tectónica: Valle de Aburrá, Cordillera Central de Colombia* [Bachelor Thesis]. Universidad EAFIT.

Arboleda, M., Arbeláez, C., Noriega-Londoño, S., & Marín-Cerón, M. (2019). Evidencias del control tectónico en la evolución del Valle de Aburrá: implicaciones a partir de análisis geomorfométricos y morfoestructurales. *XVII Congreso Colombiano de Geología. IV Simposio de Exploradores*.

Arias, A. (1995). El relieve de la zona central de Antioquia: Un palimsesto de eventos tectónicos y climáticos. *Revista Facultad de Ingeniería: Universidad de Antioquia*, (10), 9-24. https://revistas.udea.edu.co/index.php/ingenieria/article/view/325539

Arias, L. A. (1996). Altiplanos y cañones en Antioquia: Una mirada genética. *Revista Facultad de Ingeniería: Universidad de Antioquia*, *12*, 84-96. https://revistas.udea.edu.co/index.php/ingenieria/article/view/325627

Aristizábal, E., & Yokota, S. (2008). Evolución geomorfológica del Valle de Aburrá y sus implicaciones en la ocurrencia de movimientos en masa. *Boletín de Ciencias de La Tierra*, (24), 2008. https://revistas.unal.edu.co/index.php/rbct/article/view/9268

Aristizábal, E., Yokota, S., Ohira, H., & Hagai, J. (2004). Dating of slope sdiments and alluvial deposits in the Aburra Valley, Colombia. *Geoscience Reports of Shimane University*, *23*, 85-88. https://ir.lib.shimane-u.ac.jp/6148

Bilardello, D. (2016). Magnetic Anisotropy: Theory, Instrumentation, and Techniques. In *Reference Module in Earth Systems and Environmental Sciences*. https://doi.org/10.1016/B978-0-12-409548-9.09516-6

Borradaile, G. J., & Henry, B. (1997). Tectonic applications of magnetic susceptibility and its anisotropy. *Earth-Science Reviews*, *42*(1-2), 49-93. https://doi.org/10.1016/S0012-8252(96)00044-X

Borradaile, G. J. (1988). Magnetic susceptibility, petrofabrics and strain. *Tectonophysics*, *156*(1-2), 1-20. https://doi.org/10.1016/0040-1951(88)90279-X

Botero, G. (1963). *Contribución al conocimiento de la geología de la zona central de Antioquia*. Universidad Nacional de Colombia.

Burbank, D. W., & Anderson, R. S. (2011). *Tectonic Geomorphology*. John Wiley & Sons, Ltd. https://doi.org/10.1002/9781444345063

Busby, C. J., & Bassett, K. N. (2007). Volcanic facies architecture of an intra-arc strike-slip basin, Santa Rita Mountains, Southern Arizona. *Bulletin of Volcanology*, *70*(1), 85-103. https://doi.org/10.1007/s00445-007-0122-9

Caballero Acosta, J. H. (2014). Important forgotten earthquakes for Medellin. *Boletín de Ciencias de La Tierra*, (36), 69-70. https://doi.org/10.15446/rbct.n36.47639

Caricchi, C., Cifelli, F., Kissel, C., Sagnotti, L., & Mattei, M. (2016). Distinct magnetic fabric in weakly deformed sediments from extensional basins and fold-and-thrust structures in the Northern Apennine orogenic belt (Italy). *Tectonics*, *35*(2), 238-256. https://doi.org/10.1002/2015TC003940

Casas-Sainz, A. M., Gil-Imaz, A., Simón, J. L., Izquierdo-Llavall, E., Aldega, L., Román-Berdiel, T., Osácar, M. C., Pueyo-Anchuela, Ó., Ansón, M., García-Lasanta, C., Corrado, S., Invernizzi, C., & Caricchi, C. (2018). Strain indicators and magnetic fabric in intraplate fault zones: Case study of Daroca thrust, Iberian Chain, Spain. *Tectonophysics*, *730*, 29-47. https://doi.org/10.1016/j.tecto.2018.02.013

Chadima, M., & Jelinek, V. (2019). *Anisoft5.1.03: Anisotropy data browser for Windows*. Agico, Inc.

Chicangana, G. (2005). The Romeral fault system: a shear and deformed extinct subduction zone between oceanic and continental lithospheres in Northwestern South America. *Earth Sciences Research Journal*, *9*(1), 51-66.

Cho, H., Kim, M.-C., Kim, H., & Son, M. (2014). Anisotropy of Magnetic Susceptibility (AMS) of the Quaternary Faults, SE Korea: Application to the Determination of Fault Slip Sense and Paleo-stress Field. *The Journal of the Petrological Society of Korea*, *23*(2), 75-103. https://doi.org/10.7854/JPSK.2014.23.2.75

Cifelli, F., Mattei, M., Hirt, A. M., & Günther, A. (2004). The origin of tectonic fabrics in "undeformed" clays: the early stages of deformation in extensional sedimentary basins. *Geophysical Research Letters*, *31*(9). https://doi.org/10.1029/2004GL019609

Cloos, H. (1928). Experimente zur inneren tektonik. *Centralblatt Für Mineralogie*, *1*, 609-621.

Correa-Martínez, A., Martens, U., & García, G. (2020). Collage of tectonic slivers abutting the eastern Romeral Fault System in central Colombia. *Journal of South American Earth Sciences*, *104*, 102794. https://doi.org/10.1016/j.jsames.2020.102794

Cosgrove, J. W. (2007). The use of shear zones and related structures as kinematic indicators: A review. In *Deformation of the Continental Crust: The Legacy of Mike Coward*. Geological Society Special Publication, vol. 272. https://doi.org/10.1144/GSL.SP.2007.272.01.05

Costa, C., Alvarado, A., Audemard, F., Audin, L., Benavente Escóbar, C., Bezerra, F., Cembrano, J., González, G., López, M., Minaya, E., Santibáñez, I., García Peláez, J. A., Arcila, M., Pagani, M., Pérez, I., Delgado, F., Paolini, M., & Garro, H. (2020). Hazardous faults of South America; compilation and overview. *Journal of South American Earth Sciences*, *104*, 102837. https://doi.org/10.1016/j.jsames.2020.102837

Davis, G. H., Bump, A. P., García, P. E., & Ahlgren, S. G. (2000). Conjugate Riedel deformation band shear zones. *Journal of Structural Geology*, *22*(2), 169-190. https://doi.org/10.1016/S0191-8141(99)00140-6

Ego, F., Sébrier, M., & Yepes, H. (1996). Is the Cauca-Patia and Romeral Fault System left or right lateral? *Geophysi-*

cal Research Letters, *22*(1), 33-36. https://doi.org/10.1029/94GL02837

Espinosa, A. (2003). La sismicidad histórica en Colombia. *Revista Geográfica Venezolana*, *44*(2), 271-283. http://ecotropicos.saber.ula.ve/db/ssaber/Edocs/pubelectronicas/revistageografica/vol44num2/nota42-2-1.pdf

Gallego, A., Ospina, L., & Osorio, J. (2005). Sismo del Quindío del 25 de enero de 1999, evaluación morfotectónica y sismológica. *Boletín de Geología*, *27*(1), 134-150. https://revistas.uis.edu.co/index.php/revistaboletindegeologia/article/view/869

Gallego, J. (2018). *Assessment of recent tectonic activity of the Sabanalarga Fault System, Western Antioquia – Colombia* [Master thesis]. University of Bern.

García, C. (2006). Estado del conocimiento de los depósitos de vertiente del Valle de Aburrá. *Boletín de Ciencias de La Tierra*, (19). https://revistas.unal.edu.co/index.php/rbct/article/view/724

García, Y. C., Martínez, J. I., Vélez, M. I., Yokoyama, Y., Battarbee, R. W., & Suter, F. D. (2011). Palynofacies analysis of the late Holocene San Nicolás terrace of the Cauca paleolake and paleohydrology of northern South America. *Palaeogeography, Palaeoclimatology, Palaeoecology*, *299*(1-2), 298-308. https://doi.org/10.1016/j.palaeo.2010.11.010

Gómez-Tapias, J., Nivia, Á., Montes, N. E., Almanza, M. F., Alcárcel, F. A., & Madrid, C. (2015). *Notas explicativas: Mapa geológico de Colombia*. Publicaciones Geológicas Especiales *33*. Servicio Geológico Colombiano.

Gürbüz, A. (2010). Geometric characteristics of pull-apart basins. *Lithosphere*, *2*(3), 199-206. https://doi.org/10.1130/L36.1

Hamilton, T. D., Borradaile, G. J., & Lagroix, F. (2004). Sub-fabric identification by standardization of AMS: an example of inferred neotectonic structures from Cyprus. In *Magnetic Fabric: Methods and Applications*. Special Publications vol. 238. Geological Society of London. https://doi.org/10.1144/GSL.SP.2004.238.01.27

Henao Casas, J., & Monsalve, G. (2017). Geological inferences about the upper crustal configuration of the Medellin – Aburra valley (Colombia) using strong motion seismic records. *Geodesy and Geodynamics*, *8*(5), 319-327. https://doi.org/10.1016/j.geog.2017.07.002

Hermelin, M. (1982). El origen del valle de Aburrá: evolución de ideas. *Boletín de Ciencias de La Tierra*, (7-8), 47-65. https://revistas.unal.edu.co/index.php/rbct/article/view/94642

Hermelin, M. (1992). Los suelos del oriente antioqueno: un recurso no renovable. *Bulletin De L'institut Francais D'etu-*

des Andines, *21*(1), 25-36. https://www.persee.fr/doc/bifea_0303-7495_1992_num_21_1_1054

Ibáñez-Mejía, M., Restrepo, J., & García-Casco, A. (2020). Tectonic juxtaposition of Triassic and Cretaceous meta-(ultra)mafic complexes in the Central Cordillera of Colombia (Medellin area) revealed by zircon U-Pb geochronology and Lu-Hf isotopes (pp. 418-443). In *Geocronologia e Evolução Tectônica do Continente Sul-Americano: a contribuição de Umberto Giuseppe Cordani*. Solaris.

Integral. (1982). Aprovechamiento multiple del Rio Grande. Estudio geologico y evaluacion preliminar del riesgo sismico.

Integral. (2000). Conexión Túnel Aburrá Oriente. Informe geológico final.

Jelinek, V. (1977). *The statistical theory of measuring anisotropy of magnetic susceptibility of rocks and its application*. Geofyzika Brno.

Jelinek, V. (1981). Characterization of the magnetic fabric of rocks. *Tectonophysics*, *79*(3-4), T63-T67. https://doi.org/10.1016/0040-1951(81)90110-4

Kim, Y.-S., & Sanderson, D. J. (2006). Structural similarity and variety at the tips in a wide range of strike–slip faults: a review. *Terra Nova*, *18*(5), 330-344. https://doi.org/10.1111/j.1365-3121.2006.00697.x

Kirby, S. H. (2016). Active tectonic and volcanic mountain building as agents of rapid environmental changes and increased orchid diversity and long-distance orchid dispersal in the tropical Americas: opportunities and challenges. *Lankesteriana: International Journal on Orchidology*, *16*(2), 243-254. https://doi.org/10.15517/lank.v16i2.26027

Lalinde, C., González, A., & Caballero, H. (2009). Evidencia paleosísmica en el segmento de falla Sopetrán o San Jerónimo Segmento 5. *Boletín de Geología*, *31*(2), 23-34. https://revistas.uis.edu.co/index.php/revistaboletindegeologia/article/view/347

Levi, T., Weinberger, R., Alsop, G. I., & Marco, S. (2018). Characterizing seismites with anisotropy of magnetic susceptibility. *Geology*, *46*(9), 827-830. https://doi.org/10.1130/G45120.1

Levi, T., Weinberger, R., & Marco, S. (2014). Magnetic fabrics induced by dynamic faulting reveal damage zone sizes in soft rocks, Dead Sea basin. *Geophysical Journal International*, *199*(2), 1214-1229. https://doi.org/10.1093/gji/ggu300

Lomnitz, C., & Hashizume, M. (1985). The Popayán, Colombia, earthquake of 31 March 1983. *Bulletin of the Seismological Society of America*, *75*(5), 1315-1326. https://doi.org/10.1785/BSSA0750051315

Maffione, M., Pucci, S., Sagnotti, L., & Speranza, F. (2012). Magnetic fabric of Pleistocene continental clays from the hanging-wall of an active low-angle normal fault (Altotiberina Fault, Italy). *International Journal of Earth Sciences*, (101), 849-861. https://doi.org/10.1007/s00531-011-0704-9

Mann, P., Hempton, M. R., Bradley, D. C., & Burke, K. (1983). Development of pull-apart basins. *The Journal of Geology*, *91*(5), 529-554. https://doi.org/10.1086/628803

McCalpin, J. P. (2012). Paleoseismology, Second Edition. *Environmental & Engineering Geoscience*, *18*(3), 311-312. https://doi.org/10.2113/gseegeosci.18.3.311

McCalpin, J. P. (2013). Neotectonics. In *Encyclopedia of Earth Sciences Series*. Springer. https://doi.org/10.1007/978-1-4020-4399-4_252

Mejía, M., Álvarez, E., González, H. & Grosse, E. (1983). Geología de la Plancha 146 Medellin Occidental. Mapa a escala 1:100.000. Ingeominas

Mora-Páez, H., Kellogg, J. N., & Freymueller, J. T. (2020). Contributions of space geodesy for geodynamic studies in Colombia: 1988 to 2017. In Gómez, J. & Pinilla-Pachón, A. O. (eds.), *The Geology of Colombia*, vol. 4 Quaternary. Publicaciones Geológicas Especiales 38. Servicio Geológico Colombiano. https://doi.org/10.32685/pub.esp.38.2019.14

Noda, A. (2013). Strike-Slip Basin – Its Configuration and Sedimentary Facies. In *Mechanism of Sedimentary Basin Formation - Multidisciplinary Approach on Active Plate Margins*. IntechOpen. https://doi.org/10.5772/56593

Ojeda, A., & Havskov, J. (2001). Crustal structure and local seismicity in Colombia. *Journal of Seismology*, *5*(4), 575-593. https://doi.org/10.1023/A:1012053206408

Ortiz, E. A. (2002). *Evaluation of Neotectonic Activity of the Cauca-Romeral Fault System near western Medellín, Colombia* [Bachelor Thesis]. Shimane Univerity.

Page, W., & James, M. (1981). The Antiquity of the erosion surfaces and the Late Cenozoic deposits near Medellin, Colombia: implications to tectonics and erosion rates. *Revista CIAF*, *6*(1-3), 421-454.

Parés, J. (2015). Sixty years of anisotropy of magnetic susceptibility in deformed sedimentary rocks. *Frontiers in Earth Science*. https://www.frontiersin.org/article/10.3389/feart.2015.00004

Parés, J., & Pluijm, B. A. (2002). Evaluating magnetic lineations (AMS) in deformed rocks. *Tectonophysics*, *350*(4), 283-298. https://doi.org/10.1016/S0040-1951(02)00119-1

Paris, G., Machette, M. N., Dart, R. L., & Haller, K. M. (2000). Map and Database of Quaternary Faults and Folds in Colombia and its Offshore Regions. *USGS Open-File Report 2000-284*. https://doi.org/10.3133/ofr00284

Passchier, C. W., & Trouw, R. A. J. (2005). *Microtectonics*. Springer. https://doi.org/10.1007/3-540-29359-0

Poveda, E. (2013). *Discontinuidades sísmicas en la litósfera bajo la zona andina y el occidente colombianos a partir de formas de onda de sismos distantes*. Universidad Nacional de Colombia.

Ramsay, J. G. (1980). Shear zone geometry: A review. *Journal of Structural Geology*, *2*(1-2), 83-99. https://doi.org/10.1016/0191-8141(80)90038-3

Rendón, A., Gallego, J., Jaramillo, J. P., González, A., Caballero, J., Lalinde, C., & Arias, L. A. (2015). Actividad neotectónica y análisis paleosismológico en el oriente cercano a la ciudad de Medellín – Colombia. *Boletín de Ciencias de La Tierra*, *37*, 5-19.

Rendón, D. (2003). *Tectonic and sedimentary evolution of the upper Aburrá Valley, northern Colombian Andes* [Master Thesis]. Shimane University.

Rendón, D., Toro, G., & Hermelin, M. (2006). Modelo cronoestratigráfico para el emplazamiento de los depósitos de vertiente en el Valle de Aburra. *Boletín de Ciencias de La Tierra*, (18), 103-118. https://revistas.unal.edu.co/index.php/rbct/article/view/95934

Restrepo-Moreno, S., Foster, D., Stockli, D., & Parra, N. (2009). Long-term erosion and exhumation of the "Altiplano Antioqueño", Northern Andes (Colombia) from apatite (U–Th)/He thermochronology. *Earth and Planetary Science Letters*, *278*(1-2), 1-12. https://doi.org/10.1016/j.epsl.2008.09.037

Restrepo, J. (1991). *Datación de algunas cenizas volcánicas de Antioquia por el método de trazas de fisión*. AGID Report 16. Universidad EAFIT.

Riedel, W. (1929). Zur Mechanik geologischer Brucherscheinungen. *Zentralblatt Für Mineralogie, Geologie, Und Paleontologie*, 354.

Rodríguez, G., Zapata, G., González, H. & Cossio, U. (2005). *Geología de la Plancha 147 Medellín Oriental. Mapa a escala 1:100.000*. Ingeominas

Schwanghart, W., & Scherler, D. (2014). Short Communication: TopoToolbox 2 - MATLAB-based software for topographic analysis and modeling in Earth surface sciences. *Earth Surface Dynamics*, *2*, 1-7. https://doi.org/10.5194/esurf-2-1-2014

SGM. (2002). *Microzonificación sísmica de los municipios del Valle de Aburrá y definición de zonas de riesgo por movimientos en masa e inundaciones*.

Shlemon, R. (1979). Zonas de deslizamientos en los alrededores de Medellín, Antioquia (Colombia). Ingeominas.

Silva, D. (1999). *Datación por trazas de las tefras depositadas en los alrededores del Valle de Aburrá* [Bachelor Thesis]. Universidad EAFIT.

Soto, R., Larrasoaña, J. C., Arlegui, L. E., Beamud, E., Oliva-Urcia, B., & Simón, J. L. (2009). Reliability of magnetic fabric of weakly deformed mudrocks as a palaeostress indicator in compressive settings. *Journal of Structural Geology*, *31*(5), 512-522. https://doi.org/10.1016/j.jsg.2009.03.006

Stewart, I. (2005). Neotectonics. *Encyclopedia of Geology*, 425-428. https://doi.org/10.1016/B0-12-369396-9/00502-5

Suter, F., Martínez, J. I., & Vélez, M. I. (2011). Holocene soft-sediment deformation of the Santa Fe–Sopetrán Basin, northern Colombian Andes: Evidence for pre-Hispanic seismic activity? *Sedimentary Geology*, *235*(3-4), 188-199. https://doi.org/10.1016/j.sedgeo.2010.09.018

Toro, G. (1999). *Tëphrocronologie de la Colombie centrale (département d´Antioquia et abanico de Pereira)* [Ph.D. Thesis]. Université Joseph Fourier.

Toro, G., Hermelin, M., Schwabe, E., Posada, B. O., Silva, D., & Poupeau, G. (2006). Fission-track datings and geomorphic evidences for long-term stability in the Central Cordillera highlands, Colombia. *Zeitschrift Fur Geomorphologie, Supplementband*.

Traforti, A., Massironi, M., & Zampieri, D. (2016). Geo-structural map of the Laguna Blanca basin (Southern Central Andes, Catamarca, Argentina). *Journal of Maps*, *12*(3), 431-442. https://doi.org/10.1080/17445647.2015.1035557

Veloza, G., Styron, R., & Taylor, M. (2012). Open-source archive of active faults for northwest South America. *GSA Today*, *22*(10), 4-10. https://doi.org/10.1130/GSAT-G156A.1

Vinasco, C. (2019). The romeral shear zone. In *Frontiers in Earth Sciences*. https://doi.org/10.1007/978-3-319-76132-9_12

Vinasco, C., & Cordani, U. (2012). Reactivation episodes of the Romeral fault system in the Northwestern part of Central Andes, Colombia, through 39AR-40AR and K-AR results. *Boletín de Ciencias de La Tierra*, (32), 111-124. https://revistas.unal.edu.co/index.php/rbct/issue/view/3449

Weil, A., & Yonkee, A. (2009). Anisotropy of magnetic susceptibility in weakly deformed red beds from the Wyoming salient, Sevier thrust belt: Relations to layer-parallel shortening and orogenic curvature. *Lithosphere*, *1*(4), 235-256. https://doi.org/10.1130/L42.1

Wilches-Chaux, G. (2005). El terremoto, la avalancha y los deslizamientos de la cuenca del río Páez (Cauca), 1994. *Desastres de Origen Natural En Colombia 1979-2004*, 121-133.

Yokota, S., & Ortíz, E. A. (2003). 14C dating of an organic paleosol covering gravel beds distributed along the San Jerónimo Fault, Western Medellín, Colombia. *Geoscience Reports of Shimane University*, *22*, 179-182.